

Short Communication

## Effects of Additive for Anodizing Electrolyte on Anodic Film of High Silicon Aluminum Alloy

Yan Shang<sup>1,2</sup>, Linshan Wang<sup>1,\*</sup>, Dun Niu<sup>1</sup>, Zhaoyue Liu<sup>1</sup>, Yuhong Wang<sup>1</sup>, Changsheng Liu<sup>2</sup>

<sup>1</sup> College of Science, Northeastern University, Shenyang 110819, P. R. China.

<sup>2</sup> Key Laboratory of Anisotropy and Texture of Materials, Ministry of Education, Northeastern University, Shenyang 110819, P. R. China.

\*E-mail: [lswang@mail.neu.edu.cn](mailto:lswang@mail.neu.edu.cn)

Received: 12 November 2015 / Accepted: 9 December 2015 / Published: 1 January 2016

---

High silicon aluminum alloy, Al-12.7Si-0.7Mg, is newly developed and in urgent need of surface treatment techniques. Sulfuric acid concentration, anodization temperature, anodization time and current density being fixed, three kinds of organic acids were investigated as additives of electrolytes for anodic oxidation of high silicon aluminum alloy. Optimal concentrations of organic acids were worked out by inspecting their effect on film weight and corrosion time, respectively. The study showed that citric acid was the best additive. Voltage-time curves of anodic oxidation for high silicon aluminum alloy in different electrolytes conformed to the typical characteristic curve of aluminum anodic oxidation. Oxide films obtained from sulfuric-citric mixed acid electrolyte were smooth, well-distributed, compact, and exhibited exceedingly low corrosion rate and excellent corrosion resistance.

---

**Keywords:** Al-12.7Si-0.7Mg alloy; anodizing; organic acid; performance

### 1. INTRODUCTION

Comparing with other traditional materials, high silicon aluminum alloy exhibits a multitude of outstanding features, such as low density, high strength, small linear expansion coefficient, good dimensional stability, castability and machinability. Due to these superior characteristics, high silicon aluminum alloy are used widely as environmentally friendly structural materials for ships, airplanes and automobiles [1-3]. Al-12.7Si-0.7Mg is a novelly developed magnesium containing high silicon aluminum alloy extrusion profile, possessing better yield strength and similar extensibility compared with commercial 6xxx series aluminum alloys [4,5]. Nevertheless, surface treatment techniques are urgently in need for these alloys with excellent mechanical properties and broad market prospects.

To date, anodizing is the most widespread method for the treatment of aluminum alloy surface in industry. Two contrary processes are involved in anodic oxidation of aluminum alloys, i.e. Al dissolves from and  $\text{Al}_2\text{O}_3$  generates on the alloy surface, forming a micron-size film of  $\text{Al}_2\text{O}_3$  as a result [6-10]. Anodic oxide films can promote hardness and corrosion resistance of aluminum alloy surface. According to numerous of previous studies, researchers poured attention into processing parameters of the anodic oxidation treatment, e.g. anodizing temperature [11], direct current (DC) voltage [12], current density, concentration of electrolytes, and anodizing time [13]. However, few studies on organic acids as additives of anodizing electrolytes have been reported. Organic acids may improve the corrosion resistance, abrasion resistance and electrical insulation of oxide films, increase the film thickness as well [14-16]. Therefore, it is an interesting area to research on organic acids as additives of electrolytes for anodizing of high silicon aluminum alloy.

In this work, three kinds of organic acids were investigated as additives of electrolytes for anodic oxidation of Al-12.7Si-0.7Mg alloy, with fixed sulfuric acid concentration, anodization temperature, anodization time and current density. The effect of organic acid types and doses on oxide film weight and corrosion time was explored. Potassium dichromate spot test, neutral salt spray test, alkaline etching test and electrochemical measurement were used to research the corrosion resistance of the anodization films.

## 2. MATERIALS AND METHODS

### 2.1 Materials

The composition of alloy is wt%: 12.7 Si, 0.7 Mg, 0.3 Fe, 1.5 Cu, 0.3 Ni, 0.3 Ti and bal. Al. The Al-12.7Si-0.7Mg alloys were cut into  $32 \times 30 \times 3.8$  mm as test samples. Sulfuric acid, oxalic acid, citric acid, tartaric acid and other chemical reagents were of analytical purity. Deionized water was used as solvent.

### 2.2 Technological process

The technological process of preparing anodic layers comprised materials pre-treatment, anodic oxidation and hole sealing post-treatment. In order to prepare excellent anodic oxide films, pretreatment was a key step to remove impurities, oil stain and natural oxide film on alloy surface. The pretreatment of samples included mechanical polishing, deoil, caustic wash, acidic wash and bright dipping [17]. Sulfuric acid with fixed concentration was used as dominant component of anodizing electrolyte, while anodizing temperature, time and current density was identified. Three kinds of organic acids were chosen as additives of anodizing electrolyte and their effect on the oxide films' quality and growth were discussed. Processing parameters for anodic oxidation were  $170 \text{ g}\cdot\text{L}^{-1}$  of  $\text{H}_2\text{SO}_4$ ,  $20^\circ\text{C}$  of temperature, 25 min of time and  $1.5 \text{ A}\cdot\text{dm}^{-2}$  of current density. Concentration ranges of three organic acids were all from  $5 \text{ g}\cdot\text{L}^{-1}$  to  $20 \text{ g}\cdot\text{L}^{-1}$ . After anodic oxidation, all samples were sealed in boiling deionized water for 40 min, and then rinsed with ethyl alcohol and dried in warm air.

### 2.3 Characterization of oxide films

Anodic oxide films were detected by alkaline etching test (JIS H 8681-1:1999), neutral salt spray test (NSS, GB/T 10125-1997 and GB/T 6461-2002) and potassium dichromate spot test (SJ1276-77). Microstructure of anodic oxide films was observed by (SSX-550, Shimadzu Corporation, Japan) Scanning electron microscope (SEM), Energy dispersive spectroscopy (EDS) and (D/max-rA, Rigaku Company, Japan) X-Ray diffraction (XRD) analysis. The polarization curves were measured in 3.5 wt% NaCl aqueous solution on a CHI600D electrochemical workstation (Shanghai CH Instruments) in a three-electrode system, test sample as working electrode, platinum stick as counter electrode, and saturated calomel electrode (SCE) as reference electrode. Polarization curves were measured with respect to the open circuit potential at a scanning rate of  $5 \text{ mV}\cdot\text{s}^{-1}$ .

The mass of alumina per unit area ( $\text{mg}\cdot\text{dm}^{-2}$ ) on sample surface was referred to as film weight, which was determined by ASTM B137. Corrosion time was recorded by alkaline etching test. Clean the specimen, drop the alkaline etching solution ( $100 \text{ g}\cdot\text{L}^{-1}$  NaOH) on the film surface, record the time when uniform bubbles were observed. Voltage values were recorded every two minutes during anodic oxidation process in order to draw voltage-time curves.

## 3. RESULTS AND DISCUSSION

### 3.1 Effects of three additives on anodic oxide films

In this work, sulfuric acid ( $170 \text{ g}\cdot\text{L}^{-1}$ ) was used as the primary constituent of anodizing electrolyte. Effects of different concentration of additives on the film weight and corrosion resistance were investigated. The results are shown in Fig. 1 and Fig. 2. Fig. 1 indicates that the concentration of the organic acid additives influenced the film weight. For oxalic acid additive, film weight got maximum at concentration of  $5 \text{ g}\cdot\text{L}^{-1}$ . The other two additives were  $15 \text{ g}\cdot\text{L}^{-1}$  of citric acid and  $5 \text{ g}\cdot\text{L}^{-1}$  of tartaric acid, respectively, to attain the heaviest films. Dissolution and generation of alumina were two concomitant and competitive processes during anodizing of aluminum alloys [9]. When organic acid concentrations reached above certain values, rate of dissolution of alumina was higher than that of generation, resulting in reduction of anodic oxidation film, as shown in Fig. 1.

Alkaline etching test ( $100 \text{ g}\cdot\text{L}^{-1}$  NaOH) was used to characterize the corrosion resistance of anodic oxidation film. Fig. 2 shows the influences of additives and their concentrations on corrosion resistance of anodic oxidation film. For the sample treated with  $15 \text{ g}\cdot\text{L}^{-1}$  citric acid as additive, corrosion time got a maximum of 44 s. It is easily to understand that variations of corrosion time marched well with that of film weight.

To summarize, the optimal concentration of additives was as follows:  $15 \text{ g}\cdot\text{L}^{-1}$  of citric acid,  $5 \text{ g}\cdot\text{L}^{-1}$  of oxalic acid and  $5 \text{ g}\cdot\text{L}^{-1}$  of tartaric acid, respectively.

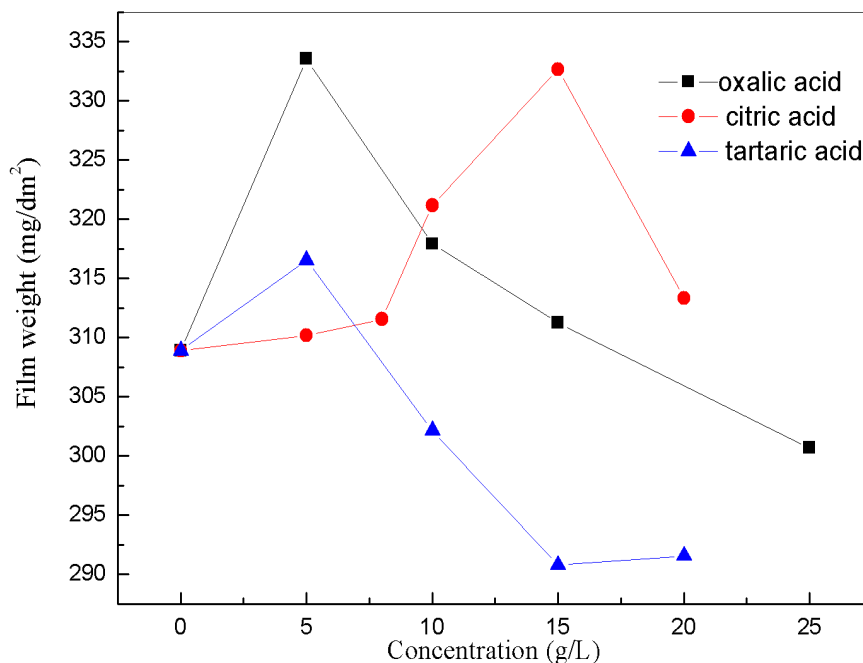


**Figure 1.** The influence of different concentration of organic acid additives on anodic oxidation film weight (anodic oxidation parameters as follows: 170 g·L<sup>-1</sup> of H<sub>2</sub>SO<sub>4</sub>, 20 °C of temperature, 25 min of time and 1.5 A·dm<sup>-2</sup> of current density).

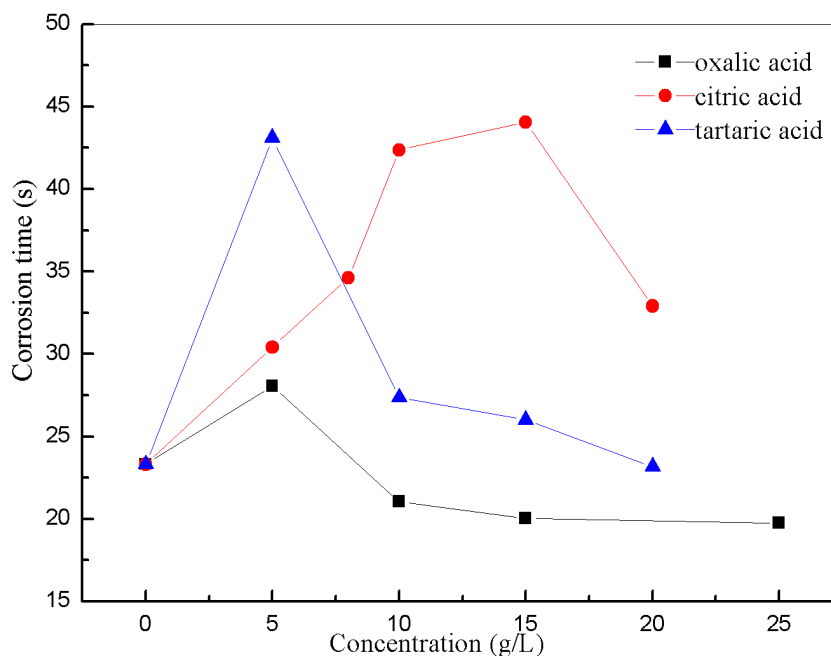


**Figure 2.** The influence of different concentration of additives on corrosion resistance of anodic oxidation film (anodic oxidation parameters as follows: 170 g·L<sup>-1</sup> of H<sub>2</sub>SO<sub>4</sub>, 20 °C of temperature, 25 min of time and 1.5 A·dm<sup>-2</sup> of current density).

### 3.2 The characteristic curve of anodic oxidation in different electrolyte

At a fixed current density of  $1.5 \text{ A} \cdot \text{dm}^{-2}$ , voltage-time curves for high silicon aluminum alloy in four kinds of electrolytes conformed to the typical characteristic curve of aluminum anodic oxidation [18,19], as shown in Fig. 3. The curves were divided into three stages. The ab stage was the formation of barrier layer and the voltage rose sharply. The formation of porous layer was in bc stage and the voltage dropped. The thickness of porous layer increased stably after point c, while voltage was basically unchanged. Thus, the shapes of voltage-time curves of three kinds of electrolyte with additives were identical with that of sulfuric acid electrolyte, indicating that additives did not change the anodic oxidation process.

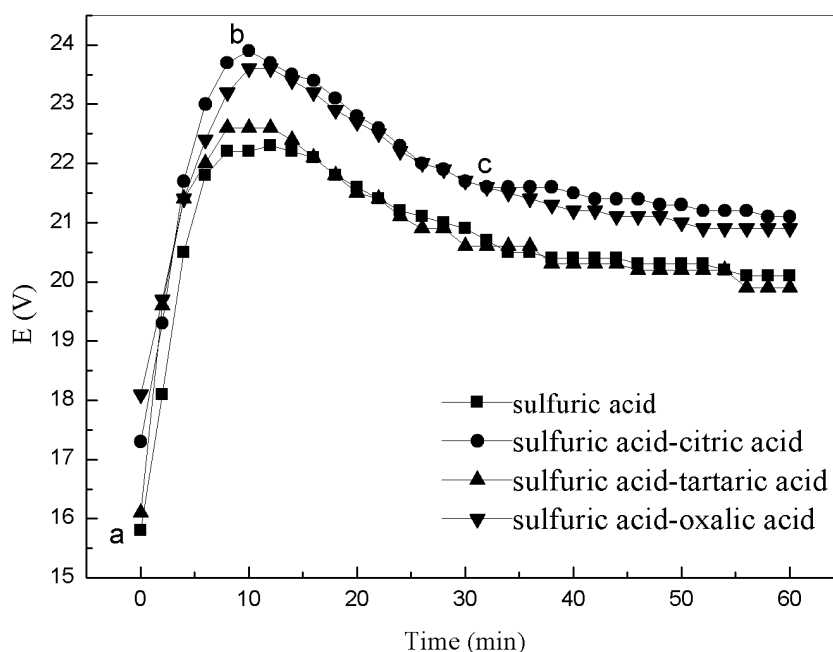


**Figure 3.** The voltage-time curves in different electrolyte at a fixed current density of  $1.5 \text{ A} \cdot \text{dm}^{-2}$ .

### 3.3 Microstructure and compositions analysis

It is well known that anodization film is composed of porous layer and block layer. The outer porous layer presents cellular structure with pseudo hexagonal prisms. These pseudo hexagonal prisms constitute numerous micro-channels, whose bottom is the inner block layer [20,21]. Porous surface formation is advantageous for further treatment after anodic oxidation, e.g., to deposit metals by carrying out alternating current (AC) electrolysis [22,23]. Fig. 4 shows SEM microcosmic pictures of anodic oxide film surface. It is indicated that the amount of micro-pore on oxide film surface (Fig 4 (a)) formed from sulfuric acid electrolyte was less than that of other films. The surface morphology of anodic oxide films generated by different electrolyte was similar. In the mixed electrolyte of sulfuric acid and citric acid, the surface of anode oxide films exhibited advantages in smoothness, well-distribution and excellent densification owing to the adding of extremely weak citric acid.

Furthermore, the addition of citric acid thickened anodic oxide film and thus improved its corrosion resistance. White particles in the SEM pictures (as shown in Fig. 4) were silicon granules which distributed evenly.

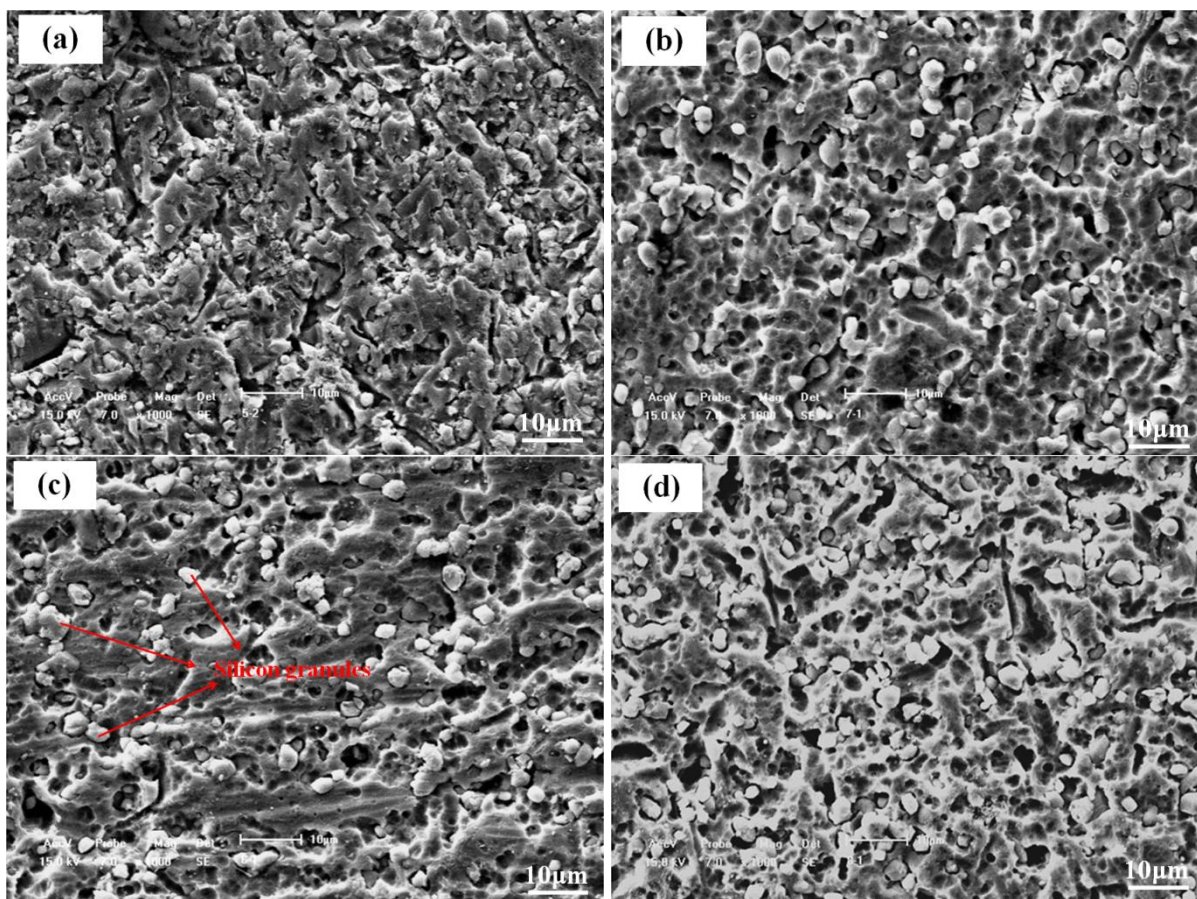


**Figure 4.** SEM micrographs of surface of anodic oxide films formed from different electrolytes ((a) sulfuric acid; (b) sulfuric-oxalate acid; (c) sulfuric-citric acid; (d) sulfuric-tartaric acid).

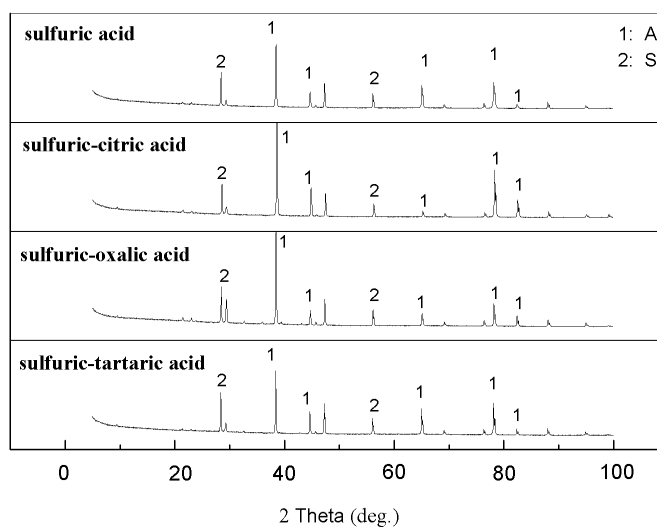


**Figure 5.** XRD pattern of anodic oxide films formed from different electrolytes

These silicon granules are alloying element to improve mechanical and casting properties of aluminum alloys. EDS analysis of the composition of different anode oxide films indicate that the anodic oxide film contained Al, Si and S elements. Fig. 5 is the X-ray diffraction pattern of alloy surface after anodizing. In agreement with EDS analysis, XRD pattern shows that the anodic oxide film contained Al and Si.

### 3.4 Corrosion resistance research

The corrosion resistance research of anodic oxide film was carried out by neutral salt spray (NSS) test, potassium dichromate spot test and electrochemical measurement (potentiodynamic polarization).

The constituents of potassium dichromate spot test were HCl (25 mL),  $K_2Cr_2O_7$  (3 g) and deionized water (75 mL). The corrosion resistance time was recorded according to the color change from orange to green. The results as listed in Table 1 showed that organic acids improved the corrosion resistance of anodic oxide film. The addition of citric acid was most conducive to the corrosion resistance of films. NSS test lasted for 240 h, and the results were also listed in Table 1. Samples made from sulfuric-citric acid electrolyte exhibited the least average corrosion rate, about  $6.0 \text{ mg}\cdot\text{h}^{-1}\cdot\text{m}^{-2}$ , indicating that citric acid was the most effective additive.

**Table 1.** The result of potassium dichromate spot test and NSS test

Sample	Potassium dichromate spot test	NSS test
	Time needed for color change (s)	Average corrosion rate ( $\text{mg}\cdot\text{h}^{-1}\cdot\text{m}^{-2}$ )
Sulfuric acid	50	9.7
Sulfuric-citric acid	68	6.0
Sulfuric-tartaric acid	53	7.5
Sulfuric-oxalic acid	60	7.3

The potentiodynamic polarization curve is a helpful tool in determining the instantaneous corrosion rate of a substrate. In a typical polarization curve, a lower corrosion current density ( $I_{\text{corr}}$ ) or a higher corrosion potential ( $E_{\text{corr}}$ ) corresponds to a lower corrosion rate and a better corrosion resistance [24]. Fig. 6 shows the polarization curves of the bare sample and anodized samples measured in solution of 3.5 wt% NaCl after immersion for 30 min. The corrosion current density, corrosion potential and corrosion rate ( $V_{\text{corr}}$ ) were calculated and given in Table 2. It can be seen that all oxidation films showed better corrosion resistance than naked sample, due to their higher corrosion potentials and less corrosion current densities. In this study, the corrosion potential of anodized films could reach about -0.45, -0.65, -0.65 and -0.67 V, respectively. Furthermore, the corrosion current of oxidation films obviously decreased because of addition of organic acid additives in electrolytes. The corrosion current density of film formed from sulfuric-citric acid electrolyte was  $5.01 \times 10^{-9} \text{ A}\cdot\text{cm}^{-2}$ ,

only about one thousandth of that of naked sample ( $7.94 \times 10^{-6} \text{ A}\cdot\text{cm}^{-2}$ ) and about a quarter of that of sulfuric acid oxidation film ( $1.99 \times 10^{-8} \text{ A}\cdot\text{cm}^{-2}$ ). Compared with other two additives, citric acid was the most effective in reducing corrosion rate of oxidation films.

According to the results of NSS test, potassium dichromate spot test and potentiodynamic polarization, anodized film obtained in sulfuric-citric acid electrolyte proved wonderful corrosion resistance. Moreover, the corrosion resistance research indicated that the anodized layers could significantly improve the corrosion resistance of high silicon aluminum alloy, Al-12.7Si-0.7Mg.

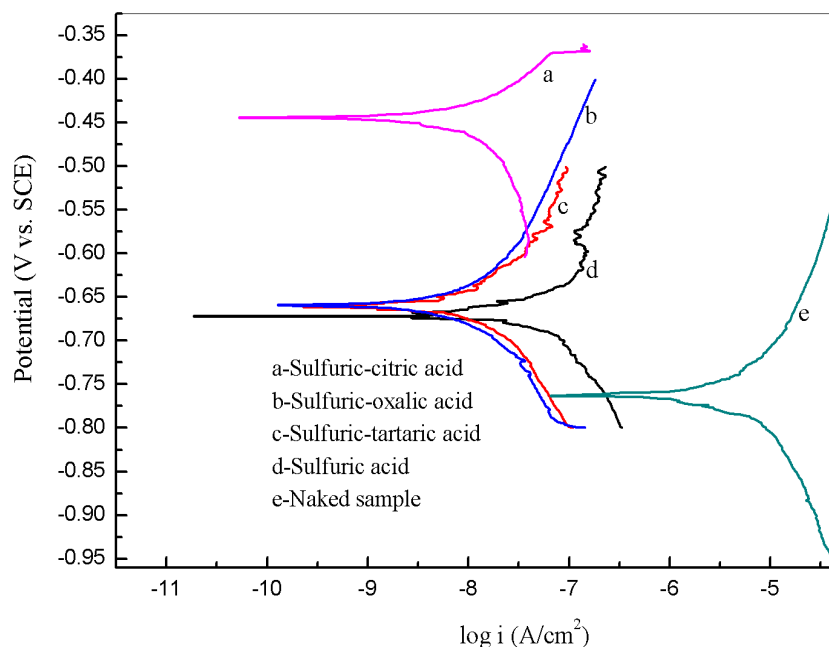


**Figure 6.** Polarization curves of the naked sample and the anodized layers in 3.5 wt% NaCl solution (a-sulfuric-citric acid; b-sulfuric-oxalic acid; c-sulfuric-tartaric acid; d-sulfuric acid; e-naked sample).

**Table 2.** Corrosion potential, corrosion current, corrosion rate of different samples.

Sample	$E_{\text{corr}}$ (V vs.SCE)	$I_{\text{corr}}$ ( $\text{A}\cdot\text{cm}^{-2}$ )	$V_{\text{corr}}$ ( $\text{mm}\cdot\text{a}^{-1}$ )
Naked sample	-0.76	$7.94 \times 10^{-6}$	$9.29 \times 10^{-2}$
Sulfuric acid	-0.67	$1.99 \times 10^{-8}$	$2.33 \times 10^{-4}$
Sulfuric-citric acid	-0.45	$5.01 \times 10^{-9}$	$5.86 \times 10^{-5}$
Sulfuric-tartaric acid	-0.65	$6.31 \times 10^{-9}$	$7.38 \times 10^{-5}$
Sulfuric-oxalic acid	-0.65	$7.94 \times 10^{-9}$	$9.29 \times 10^{-5}$

#### 4. CONCLUSIONS

Based on data of oxidation film weights and corrosion times, the optimal concentrations of additives were determined as follows:  $15 \text{ g}\cdot\text{L}^{-1}$  of citric acid,  $5 \text{ g}\cdot\text{L}^{-1}$  of oxalic acid,  $5 \text{ g}\cdot\text{L}^{-1}$  of tartaric



acid. Voltage-time curves for high silicon aluminum alloy in different electrolytes conformed to the typical characteristic curve of aluminum anodic oxidation. Formed in the mixed electrolyte of sulfuric acid and citric acid, the surface of anode oxide films exhibited advantages in smoothness, well-distribution and excellent densification compared with the other films. EDS analysis and XRD pattern demonstrated the anodic oxide film contained Al and Si. The results of NSS test, potassium dichromate spot test and potentiodynamic polarization indicated that citric acid was the most effective additive for enhancing corrosion resistance of anodic oxidation film for high silicon aluminum alloy.

#### ACKNOWLEDGEMENT

This research was financially supported by the Projects in the National Science & Technology Pillar Program of China (2009BAE80B01) and by the Fundamental Research Funds for the Central Universities (N120610003).

#### References

1. V. Vijeesh, K. Narayan Prabhu, *Trans. Indian Inst. Met.*, 67(1) (2014) 1–18.
2. L.P. Troeger, E.A. Starke Jr, *Mat. Sci. Eng. A*, 277 (1-2) (2000) 102.-113.
3. Z.X. Liang, B. Ye, L. Zhang, Q.G. Wang, W.Y. Yang, Q.D. Wang, *Mater. Lett.*, 97 (2013) 104–107.
4. L. Fang, Y. Fuxiao, Z. Dazhi, Z. Liang, *Mat. Sci. Eng. A*, 528 (2011) 3786-3790.
5. L. Fang, Y. Fuxiao, Z. Dazhi, Z. Liang, *Mater. Charact.*, 107 (2015) 211-219.
6. A. Pakes, G.E. Thompson, P. Skeldon, P.C. Morgan, *Corros. Sci.*, 45 (2003) 1275-1287.
7. L. Bouchama, N. Azzouz, N. Boukouche, J.P. Chopart, A.L. Daltin, Y. Bouzmit, *Surf. Coat. Tech.*, 235 (2013) 676-684.
8. G.D. Sulka, K.G. Parkola, *Electrochim. Acta*, 52(2007) 1880-1888.
9. J.P.O Sullivan, G.C. Wood, *Pro. Roy. Soc. Lond. A*, 317 (1970) 511-543.
10. J.Y. Wang, C. Li, C.Y. Yin, Y.H.Wang, S.L. Zheng, *Surf. Coat. Tech.*, 258 (2014) 615-623.
11. S. Theohari, Ch. Kontogeorgou, *Appl. Surf. Sci.*, 284 (2013) 611-618.
12. C.K. Chung, M.W. Liao, H.C. Chang, C.T. Lee, *Thin Solid Films*, 520(2011) 1554-1558.
13. W. J. Stępniewski, Z. Bojar, *Surf. Coat. Tech.*, 206 (2011) 265-272.
14. H. Lei, L. Jianhua, L. Songmei, Y. Mei, *Int. J. Electrochem. Sci.*, 10 (2015) 2194-2205.
15. W. J. Stępniewski, M. Norek, M. Michalska-Domańska, Z. Bojar, *Mater. Lett.*, 111 (2013) 20-23.
16. B. Chaolei, H. Yedong, S. Xin, *Trans. Nonferrous Met. Soc. China*, 21(2011) 133-138.
17. B. Gastón-García, E. García-Lecina, J. A. Díez, M. Belenguer, C. Müller, *Electrochem. Solid St.*, 13 (11) (2010) 33-35.
18. M. xiangfeng, W. Guoying, G. Hongliang, Y. Yundan, C. ying, H. Dettinger, *Int. J. Electrochem. Sci.*, 8 (2013) 10660-10671.
19. K. Shimizu, K. Kobayash, *Philos. Mag. A*, 66(4) (1992) 643-652.
20. H. Takahashi, M. Nagayama, *Electrochim. Acta*, 23 (3) (1978) 279-286.
21. R. Huang, K. R. Hebert, L. S. Chumbley, *J. Electrochem. Soc.*, 151(7) (2004) 379-386.
22. I. Serebrennikova, P. Vanysekt, V. I. Birss, *Electrochim. Acta*, 42(1) (1997) 145-151.
23. S. Yongqing, *Met. Finish.*, 98(12) (2000) 61-62.
24. X. Li, X. Nie, L. Wang, D.O. Northwood, *Surf. Coat. Tech.*, 200 (2005) 1994-2000.